Extraction of tumor vascularisation in fluorescent confocal microscopy

Wang Po[a] *, Catherine Kelly[b] and Sir Michael Brady[a]

[a] Wolfson Medical Vision Laboratory, University of Oxford.
[b] Gray Institute for Radiation Oncology and Biology, University of Oxford

Abstract. The aim of this work is to segment, and quantify, the vasculature of tumours, based on fluorescent microscope 3D images. Such images have poor contrast and the vascular features vary substantially within a 3D volume. In this paper, we introduce a method to estimate local phase in 3D images based on the monogenic signal theory, and illustrate its performance on our vasculature images.

1 Introduction

Tumor regions can often be characterized by malformations of their vasculature. A number of pioneering papers compare qualitatively the vasculature in tumor regions and in normal tissue [1, 2]. We have begun the development of a mathematical model both of normal vasculature and of the chaotic vasculature which is characteristic of tumors [3, 4]. With such a model in hand, we seek to fit it to the vasculature observed in images, in particular optical images. Specifically, we analyse (3D) confocal microscope images of blood vessels surrounding human head and neck tumors. Though confocal microscopy, in association with fluorescent markers, has given substantial and fresh insight into a range of biological questions, they, like all light imaging modalities, have a number of limitations and image quality remains suboptimal. Specifically in the case of our data, the images are formed in two channels, with the blood vessels and tumour cells marked separately. Because of bleed-through effect, some tumor cells also appear in the blood vessel images, obscuring the image. Inconsistencies in staining lead to heterogeneity in the signal from the vessels. Of course, mathematical model fitting, hence the accuracy of tumor vasculature quantification, depends critically on the complete and accurate detection of the blood vessels visible in the generally low contrast 3D images. It follows that image post-processing is necessary, both to restore the quality of microscopic images and to detect the vessels.

A fundamental challenge in detecting the vessels is that they are of variable thickness and do not conform to a simple intensity model such as a step or bar. Fig.1(a) shows a typical slice of the image volume. However, vessels do have a consistent appearance across a range of spatial scales, suggesting that they may be both defined and detected using the concept of phase congruency, introduced by Owens and Morrone [5]. Recognising the limitation, when applied to images, of a 1-D implementation of the phase congruency concept, Felsberg introduced the monogenic signal, based on the Riesz Transform [6] which enables rapid computation of the local energy (amplitude), local phase, and local orientation of an image at each location. Combined with a suitable family of bandpass filters, defining scale space, this enables phase congruency to be computed accurately and rapidly for images. Phase congruency based on the monogenic signal has found practical application in medical image processing, for example to enhance the contrast of blurred images [7]. Importantly, it was shown that a number of regions that did not appear clearly in the original image can have high contrast in the local phase image (Fig. 1(b)).

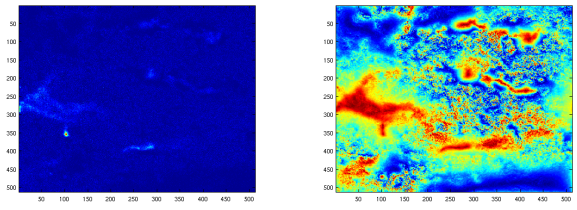

(a) original image (b) local phase image

Figure 1. 2D image slice (a) and its local phase image (b).

To both test and refine our 3D model of vasculature, we need to extend previous applications of phase congruency/monogenic signal to 3D image volumes. However, there is little discussion of the application of local phase in 3D in the literature. Hacihaliloglu et al [8] defined 3D local phase as the difference between the products of odd

*Email: wangpo@robots.ox.ac.uk

symmetrical and even symmetrical filters at different scales and orientations. This approach may be regarded as an extension to 3D of the 1D implementation of phase congruency [9], necessitating computationally costly (and inaccurate) steering in two dimensions. In contrast, we follow Felsberg's monogenic signal concept and define local phase as the angle between the real image and the imaginary components which are formed by projecting the real image onto orthogonal axes. Calculating 3D local phase using the Riesz Transform is both faster and more accurate than sequential 2D local phase calculations before 3D image construction. Though applied primarily to confocal image volumes in this paper, we contend that the method presented here has general applicability in 3D image analysis.

2 Theory

Local phase (instantaneous phase) is defined in 1D analytic signal representation as the phase between real signal and its hilbert transform. In 2D, local phase can be measured by filtering the image with 2 orthogonal odd filters and calculating the phase between the real image and the filter responses [6].

We can extend the above 2D analysis straightforwardly to 3D by filtering the 3D image volume with three orthogonal odd filters and project them into three orthogonal imaginary volumes. Local phase is then defined as the angle between the real intensity and the compound imaginary intensity:

$$\varphi(x,y,z) = atan\frac{\sqrt{(h_1 \otimes f)^2 + (h_2 \otimes f)^2 + (h_3 \otimes f)^2}}{f} \tag{1}$$

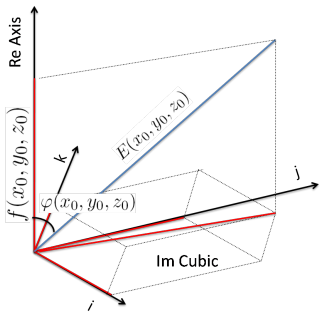

Figure 2. 3D monogenic signal: at every voxel, the intensity of the 3D monogenic signal is a vector with four components: the real intensity and three imaginary intensities. Local phase is defined as the angle between the real intensity and the compound imaginary intensity

h_1, h_2 and h_3 are the transfer functions of $-i\frac{u_1}{|u|}$, $-j\frac{u_2}{|u|}$ and $-k\frac{u_3}{|u|}$, where i, j, k are imaginary units and u_1,u_2,u_3 are basis vectors in the fourier domain. (Together with the real axis, this builds up a 4D space) Fig. 3 shows an image of sphere in 3D and the images filtered by h_1, h_2 and h_3.

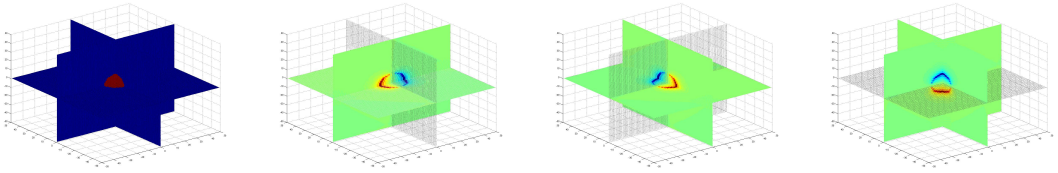

(a) Sphere (b) $f \otimes h_1$ (c) $f \otimes h_2$ (d) $f \otimes h_3$

Figure 3. Products of three orthogonal odd filters

In practice, in order to compute local phase, and specifically in order to compute phase congruency over a range of scales, images are typically pre-processed using a suitable bandpass filter g, in which case Eq.1 is actually calculated as:

$$\varphi(x,y,z) = atan\frac{\sqrt{(h_1 \otimes f_b)^2 + (h_2 \otimes f_b)^2 + (h_3 \otimes f_b)^2}}{f_b} \tag{2}$$

where $f_b = f \otimes g$ is the bandpass filtered image. There is a range of bandpass filters that one may use, including difference-of-Gaussians and log Gabor filters. Since our primary interest in this paper is to detect blood vessels, which

are typically quite narrow and give a single response rather than two step transitions of opposite sign, we have used a 3D version of the scale-invariant, localising Mellor-Brady (MB) filter [10]. The Mellor-Brady filter is defined as function of distance to the origin in spatial domain; its extension to 3D is straightforward:

$$g = \frac{A}{r^{\alpha+\beta}} - \frac{B}{r^{\alpha-\beta}} \tag{3}$$

where $r = \sqrt{x^2 + y^2 + z^2}$, α, β are scaling parameters, A,B are normalizing constants.

Local phase captures the local information of phase congruency, which is a texture identification [5]. The local phase based segmentation is thus a type of texture based segmentation, which is an accepted category of segmentation methods. Further more, as phase is intensity-invariant, it is believed to unveil the real vascular structure unaffected by the imperfectness in histochemical labelling during image acquisition process.

3 Results

As noted in the Introduction, we have applied the method developed in this paper to 3D confocal microscope images of the blood vessels surrounding human head and neck tumor tissues. These images are provided by Naseer of Gray Institute for Radiation Oncology and Biology, University of Oxford. The blood vessels are labeled with Alexa 568 (red) and images are recorded with Leica microsystems (λ_{ex} = 576nm, λ_{em} = 654nm).

The 3D volume of images are constructed and processed thereafter using ITK (Insight Toolkit) and visualized using VTK (Visualization Toolkit). Fig.4 shows the original 3D image of one sample. The red linear structure in this image represents the blood vessels. There are also several small, spherical structures which are surrounding cells. The surrounding cells are marked with GFP (Green Fluorescence Protein) and are recorded in the green channel. Because of the bleed through effect, some cells also appear in the red spectrum. For our current research, this is unwanted information. Notice that the intensity of the blood vessel is not homogeneous through its region. Also, at some blood vessel locations, the intensity is so low that purely intensity based segmentation methods are unlikely to detect the vessel.

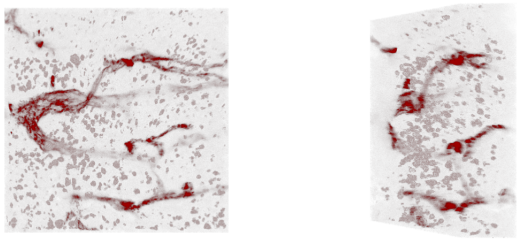

(a) view at 0° (b) view at 45°

Figure 4. Original Images of sample B

Fig. 5 shows the band-pass filtered local phase image. By band-pass filtering, the phase calculation was 'localized'. The contrast between the vessel boundary and the background is enhanced. The and the vaguely connected parts in the original image is readily recognized. We contend that this is one of the most beneficial result of phase based methods.

The band-pass filtered local phase image has greatly enhanced the contrast between objects and backgrounds. This has enabled us to utilize thresholding methods to obtain the binary representation of blood vessels. After thresholding, we used size-exclusion method to remove the unwanted smaller cell bodies by rejecting connected regions with size smaller than 2500 voxels.

Notice that in the local phase, some locations of the blood vessel still have low intensity that will be removed by rigid intensity thresholding, which causes the disjoints of the vascular structure. Disjoints produce more shorter vessel segments which may lead errors in vessel quantification. Instead, we can use the geometric information to choose which regions should be accepted as part of the blood vessel. Hysteresis thresholding utilizes two levels of thresholding. Higher level thresholding ensures the regions with high intensity be accepted as blood vessel while lower level thresholding ensures the regions with low intensity be rejected. The regions whose intensities are between the higher

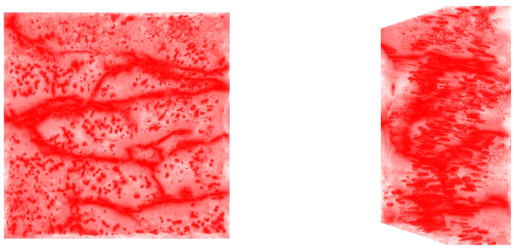

(a) view at 0° (b) view at 45°

Figure 5. 3D local phase image with band-pass filtering

level and lower level threshold will be judged based on their connectivity with the accepted vessels. Only those regions which are above the lower threshold AND are directly connected to regions above the higher threshold are accepted. This produces vascular structure with better preserved connectivity (Fig 6):

(a) view at 0° (b) view at 45°

Figure 6. 3D blood vessel image segmented using hysteresis thresholding

Skeleton is the median line of the blood vessel. The segmented image (Fig 6) could be skeletonized by 3D binary thinning algorithm, which produces the skeleton of the blood vessel (Fig 7):

(a) view at 0° (b) view at 45°

Figure 7. 3D blood vessel image skeletonized with binary thinning

By extracting skeleton of the blood vessel we can begin to calculate various geometrical parameters of the vessel structure (e.g. branching angles, inter-branch lengths, etc.) We hope we could find a pair of suitable parameters to characterize the tumor vascular structure and quantify the vacular restoration by anti-cancer drugs.

4 Conclusions

We have shown how 3D local phase image computed from a 3D fluorescent confocal image of vasculature can greatly enhance contrast and reduce noise. Instead of calculating 2D slices individually, we perform the local phase calculation directly in 3D space. In this way, the calculation is more accurate and faster. It also accentuates the connectivity, which can only be perceived vaguely in the original image.

We will apply our model [4] on the 3D digitised blood vessel network and compare the simulation results with experimental data. We will also use the method to quantitatively analyze the tumour vascular structure in different phases of anti-cancer treatment.

References

1. MA Konerding, E. Fait, and A. Gaumann. 3 D microvascular architecture of pre-cancerous lesions and invasive carcinomas of the colon. *British journal of cancer*, 84(10):1354–1362, 2001.
2. J.R. Less. Microvascular architecture in a mammary carcinoma: branching patterns and vessel dimensions. *Cancer Research*, 51(1):265–273, 1991.
3. CJ Kelly. *Quantitative Modelling of Positron Emission Tomography Tracer Kinetics in Hypoxia*. PhD thesis, University of Oxford, 2008.
4. P. Wang, CJ. Kelly, and JM. Brady. STACs - a mathematical model of the spatiotemporal distribution of dynamic PET data. In *Medical image understanding and analysis: MIUA*, volume 12, pages 79–83, 2008.
5. MC Morrone and RA Owens. Feature detection from local energy. *Pattern Recognition Letters*, 6(5):303–313, 1987.
6. M. Felsberg and G. Sommer. The monogenic signal. *Signal Processing, IEEE Transactions on [see also Acoustics, Speech, and Signal Processing, IEEE Transactions on]*, 49(12):3136–3144, 2001.
7. X. Pan, M. Brady, R. Highnam, and J. Declerck. The Use of Multi-scale Monogenic Signal on Structure Orientation Identification and Segmentation. *LECTURE NOTES IN COMPUTER SCIENCE*, 4046:601, 2006.
8. I. Hacihaliloglu, R. Abugharbieh, A. Hodgson, and R. Rohling. Bone segmentation and fracture detection in ultrasound using 3D local phase features. In *Medical image computing and computer-assisted intervention: MICCAI... International Conference on Medical Image Computing and Computer-Assisted Intervention*, volume 11, page 287. Med Image Comput Comput Assist Interv Int Conf Med Image Comput Comput Assist Interv, 2008.
9. P. Kovesi. Image features from phase congruency. *Videre: Journal of Computer Vision Research*, 1(3):1–26, 1999.
10. M. Mellor and M. Brady. Phase mutual information as a similarity measure for registration. *Medical Image Analysis*, 9(4):330–343, 2005.